



# A novel approach of lung segmentation on chest CT images using graph cuts



Shuangfeng Dai<sup>a</sup>, Ke Lu<sup>a,\*</sup>, Jiyang Dong<sup>a</sup>, Yifei Zhang<sup>a</sup>, Yong Chen<sup>b</sup>

<sup>a</sup> University of Chinese Academy of Sciences, No. 19A Yuquan Road, Beijing 100049, China

<sup>b</sup> Department of Radiology, General Hospital of Ningxia Medical University, No. 804 Shengli Street, Xingqing Area, Ningxia 750004, China

## ARTICLE INFO

### Article history:

Received 9 February 2015

Received in revised form

11 May 2015

Accepted 13 May 2015

Communicated by Yue Gao

Available online 25 May 2015

### Keywords:

Lung segmentation

Gaussian filter

Graph cuts

Gaussian mixture models

Medical image processing

## ABSTRACT

Lung segmentation is often performed as a preprocessing step on chest Computed Tomography (CT) images because it is important for identifying lung diseases in clinical evaluation. Hence, research on lung segmentation has received much attention. Most of the conventional methods need the post-processing just like rolling ball method or morphology method to deal with the juxtaleural lung nodules or other lesions. To find a most robust method of lung segmentation, we propose a new algorithm based on an improved graph cuts algorithm with Gaussian mixture models (GMMs) in this paper. The core method models the foreground object and background of the CT images as a GMMs, and the weight or probability that each pixel belongs to the foreground object is calculated with expectation maximization (EM) algorithm. The corresponding graph is then created using these weights on the nodes and edges. And the segmentation is completed with the minimum cut theory. Experimental results show that the proposed method is very accurate and efficient, and can directly provide explicit lung regions without any postprocessing operations even in complex scenarios.

© 2015 Elsevier B.V. All rights reserved.

## 1. Introduction

With the advancement of Computed Tomography (CT) technology, the amount of data obtained in clinical CT has increased exponentially. Automatic segmentation methods using computer-assisted diagnosis (CAD) have been developed, making clinical diagnosis more convenient. Lung parenchyma segmentation is a preprocessing stage in lung CT image processing, especially in the measuring and analyzing of lung disease, and the preprocessing results directly affect the subsequent image processing. Hence, faster and more accurate segmentation methods for lung CT images have been a popular subject of recent research, and could have important practical significance and clinical value.

So far, many lung segmentation methods have been studied by researchers, and the main conventional approaches include thresholding [1,2], region growing [3], watershed transform [4,5], and boundary tracking methods [6,7]. The threshold segmentation method is the traditional lung segmentation algorithm. Although the speed of threshold segmentation is fast, it is not satisfactory because the gray values of the lung area are similar to the trachea and bronchus regions. Region growing is a simple

region-based image segmentation method. It can quickly and correctly separate the interstitial lung area and maintain the border; however, the growing criterion is sensitive to parameters, and the region growing method is the time consuming. The boundary tracing method is a boundary detection method that depends on the gradient image of the original image. To some extent, boundary tracing can solve the problem of non-closed curve boundary images, but it is very sensitive to the selection of the detection point pixel, which may induce the method to follow the wrong track or interrupt the trace. Also, these methods are most likely to follow a post-processing to remove the main bronchus or separate the left/right lung. Therefore, most lung segmentation methods currently use mixed methods that are based on the threshold value method combined with regional growth and other extraction methods [7–9]. Than et al. [8] proposed an initial segmentation process that involves the Otsu grey level threshold and morphological filtering. Mansoor et al. [9] adopted a fuzzy connectedness image segmentation algorithm to perform initial lung parenchyma extraction, and used a novel neighboring anatomy-guided segmentation approach to refine it. Meng et al. [10] combined the improved live-wire model, snake model, and contour interpolation to determine the lung's contours. And many researches focus on the segmentation of lung parenchyma with lung disease. Pu et al. [11] proposed an automated lung segmentation approach based on a 2-D adaptive

\* Corresponding author.

E-mail address: [luk@ucas.ac.cn](mailto:luk@ucas.ac.cn) (K. Lu).

border marching algorithm to deal with juxta-pleural (lesions adjacent to the chest wall and mediastinum) lung nodules. Larger areas of under-segmentation were reported in hilar and pulmonary consolidation regions. Sun et al. [12] proposed a robust active shape model approach to roughly segment the outline of the lungs with lung cancer, and an optimal surface finding approach is utilized to further refine the initial segmentation result to the lung.

Because of the plasticity of the energy function and its global optimality, the graph cuts algorithm has recently rapidly developed as a new image segmentation method in graph theory. The graph cuts framework was first proposed by Boykov [13] to obtain globally optimal object segmentation in  $N$ -dimensions. Since then, the graph cuts has been quickly developed and applied in a wide range of research. Xu et al. [14] combined active contours with the graph cuts algorithm to segment objects. Yang et al. [15] analyzed the graph cuts algorithm and applied it in dense depth image for three-dimensional (3D) video. With the multi-set graph cut model, they achieved higher quality of virtual view images than the performance of the benchmark method [16]. Because some priori information can be added to the graph cuts algorithm by human interaction, which makes the graph cuts algorithm become more applicable in complex medical image segmentation [17]. Sun et al. [18] proposed an automated graph-based segmentation algorithm of lungs in 4D CT scans. He also proposed a combined framework that included a robust 3D active shape model based lung segmentation, image registration, and multi-surface (4D) optimal surface finding. Price et al. [19] proposed a method for combining geodesic distance information with edge information in a graph cuts framework to complete image segmentation. Ballangan et al. [20] used graph cuts in PET images for lung tumor segmentation, and extended the graph cuts with a standardized uptake value (SUV) cost function and a monotonic downhill SUV feature. They can get the accurate contour of lung tumors, but the time consumption is very high. Ali et al. [21] proposed a new framework for automatic lung segmentation using the graph cuts approach, they modeled the neighboring pixels with Markov Gibbs random field, and extended the energy function with Gaussian distributions and Potts distributions. They got a high accurate rate of the segmentation results and a low optimal energy. However, from the results in that paper, we can see that it also needs the post-processing to remove the main bronchus to calculate the volumes of lung. Nakagomi et al. [22] analyzed the segmentation of lung with pleural effusion using the graph cuts algorithm. They extended the graph cuts energy with multiple-shapes and neighbor structure constraints, and got a high segmentation accurate rate. But the computation time is very high, it was approximately 15–30 min per CT volume.

As discussed above, the segmentation of lung parenchyma is an initial processing step, it is very important in the clinical diagnosis. Most of the methods in the present are a combination of a variety of methods, and are time-consuming, cannot once get the segmentation result, require multiple steps. So the more robust and efficient lung segmentation methods are needed for study. Considering the research on graph cuts, which has been a hot topic and has achieved spectacular progress in recent, we present an improved graph cuts method with Gaussian mixture models (GMMs) [23,24] for lung segmentation in this paper, and the weight of each pixel that belongs to the foreground object is calculated with expectation maximization (EM) algorithm [25]. The main contribution is that the lung segmentation is obtained by the energy minimization method, which results in a corresponding reduction in the amount of calculation. With the GMMs, the segmentation can be done at one time and no need of other iteration times; the Dice similarity coefficient index is approximately 0.9874, so the segmentation is more accurate; also our proposed method can directly provide explicit lung segmentation

without any other post-processing, such as left and right lung separation. The experimental results show the accuracy and efficiency of the lung segmentation of our proposed method.

The organization of this paper is as follows: this section reviews the research related works of lung segmentation. The detailed materials and methods for graph cuts and GMMs are presented in Section 2. Section 3 presents the experimental results. Finally, the conclusion and directions for future work are given in Section 4.

## 2. Materials and methods

Lung segmentation is the basic first step for chest CT images that will be used for subsequent analysis, such as early lung disease detection or local area analysis. Therefore, to segment lung CT images more accurately, we improved the graph cuts method using GMMs in our algorithm. The steps of the overall process of our algorithm are shown in Fig. 1.

### 2.1. Gaussian smoothing

Because of the imaging machinery, environmental conditions, and other external interference, there will inevitably be noise when the CT images are created. This existing noise causes difficulties for the analysis, and it affects the segmentation accuracy of the lung region. Hence, the first step in our CT image process is to remove the noise. Commonly used CT image processing methods for noise reduction are mean, median, or Gaussian filtering. To improve the accuracy of detection and segmentation of the lung pulmonary region, the Gaussian filter with the Gaussian kernel radius  $r=0.5$  is adopted in our experiment. With that parameter, the noise of the CT images can be removed and the contour of lungs can be kept clear.

### 2.2. Graph cuts method

Graph cuts approaches have been recently applied as global optimization methods to the problem of image segmentation [13,14]. The image is represented using an adjacency graph that is set up such that every pixel is represented by a node in the graph. Each node is linked to its neighboring pixels, with the edge connecting them given a cost that is weighted by the difference in the pixel values. Two additional nodes called the source and sink nodes represent the foreground and background, respectively. Each of these nodes is connected to every pixel node. A cost is also applied to these edges according to the probability that the connected pixels value occurs in the foreground (or the background) distribution. Once the graph is set up, it is segmented by

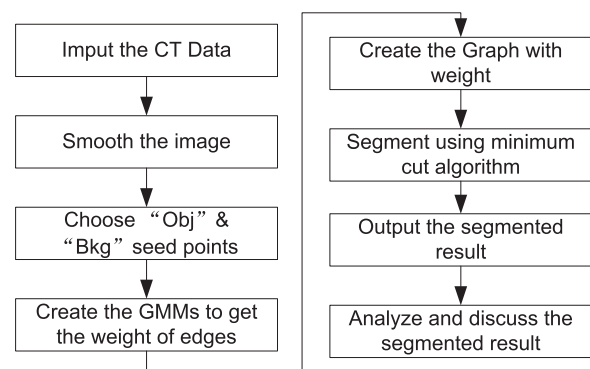


Fig. 1. Overall process of our algorithm.

performing a graph cuts using the min-cut/max-flow algorithm [17] that attempts to optimally separate the source and sink nodes (foreground and background pixels) from each other. The graph and resulting cut are shown in Fig. 2. Further detailed information on graph cuts can be found in [13].

The optimization or minimum cut criterion is defined as

$$\text{mincut}\{C_1, C_2\} = \sum_{e \in C} \omega_e \quad (1)$$

where  $C = \{C_1, C_2\}$  is a cut and  $\omega_e$  is the weight (cost) of the edges connecting  $C_1$  to  $C_2$ . Considering an arbitrary set of data elements  $P$  and some neighborhood system represented by a set  $N$  of all unordered pairs of pixels  $\{p, q\}$ , let  $A = \{A_1, \dots, A_p, \dots, A_{|P|}\}$  be a binary vector of labels and  $A_i$  is the label F or B for pixel  $p$ . Vector  $A$  defines a segmentation and can represent either the foreground object or background. Therefore, the energy function  $E(A)$  for segmentation is defined as in [13] as follows:

$$E(A) = \lambda \cdot R(A) + B(A) \quad (2)$$

where

$$R(A) = \sum_{p \in P} R_p(A_p) \quad (3)$$

$$B(A) = \sum_{\{p, q\} \in N} B_{\{p, q\}} \cdot \delta(A_p, A_q) \quad (4)$$

$$\delta(A_p, A_q) = \begin{cases} 1 & \text{if } A_p \neq A_q \\ 0 & \text{otherwise.} \end{cases} \quad (5)$$

where  $R(A)$  is a regional properties term, which assumes that the individual penalties for assigning pixel  $p$  to “obj” or “bkg” correspondingly penalty are  $R_p(\text{“obj”})$  or  $R_p(\text{“bkg”})$ .  $B(A)$  is the boundary properties term that comprises the boundary properties of segmentation  $A$ . The coefficient  $\lambda \geq 0$  in (2) specifies a relative importance of  $R(A)$  versus  $B(A)$ .

### 2.3. GMMs

In the graph cuts algorithm, the user first needs to choose the seed points for the foreground object and background region. Each seed point region is then modeled using GMMs with  $K$  subclasses. Because lung CT images are grayscale images, the value of the pixel is a number that corresponds to the intensity of the image. Let  $x$  be a random variable that takes the value. To

determine the probability model, we can suppose a mixture of Gaussian distribution of the following form [24]:

$$\Pr(x) = \sum_{k=1}^K \beta_k \cdot N(x; \mu_k, \sigma_k^2) \quad (6)$$

where  $K$  is the number of components,  $\beta$  are weights such that  $\sum_{k=1}^K \beta_k = 1$ , and  $N(\cdot)$  is the Gaussian probability density function (PDF) parameterized by mean value  $\mu_k$  and standard variance value  $\sigma_k^2$ :

$$N(\mu_k, \sigma_k^2) = \frac{1}{\sqrt{2\pi}\sigma_k} \exp\left\{-\frac{(x_i - \mu_k)^2}{2\sigma_k^2}\right\} \quad (7)$$

To perform the parameterized learning of the interactive a priori knowledge mixed model, the EM algorithm is usually the best choice. It not only provides initial robust and strong arguments, but also provides a maximum likelihood estimation. Furthermore, compared with the  $K$ -means algorithm, the EM algorithm is more suitable for graph cuts, which is just a maximized likelihood segmentation model. Here, we use the EM-MAP (Maximum a Posteriori) method [24], and the process is defined as below:

1. Initialization:  $\Theta^{(0)} = \{\beta_1^{(0)}, \dots, \beta_K^{(0)}, \mu_1^{(0)}, \dots, \mu_K^{(0)}, \sigma_1^{(0)}, \dots, \sigma_K^{(0)}\}$
2. E-step: let  $\gamma(i, k) = \beta_k \Pr(x_i | \mu_k, \sigma_k) / \sum_{j=1}^K \beta_j \Pr(x_i | \mu_j, \sigma_j)$ ;
3. M-step:  $N_k = \sum_{i=1}^N \gamma(i, k)$ ;  $\mu_k = (1/N_k) \sum_{i=1}^N \gamma(i, k) x_i$ ;  $\sigma_k = (1/N_k) \sum_{i=1}^N \gamma(i, k) (x_i - \mu_k)^2$ ;  $\beta_k = N_k/N$ ;
4. Iterate steps 2 and 3 until an arbitrary error is reached:  $e = L(\Theta)^{i+1} - L(\Theta)^i < \varepsilon$ ;
5. Calculate the final  $\Theta^*$ .

Because EM is an unsupervised parameter estimation method, the initial values of the model parameters should be given, and the methods result is sensitive to these initial values. Therefore, in the initialization step, we use the  $K$ -means clustering algorithm to determine the initial values, including mean value, variance, and weight factors. Using the above EM-MAP algorithm, we can determine the posterior probability for every interesting region in the CT image. The regional penalty  $R_p(\cdot)$  in formula (3) can then be written as follows:

$$R_p(\text{“obj”}) = -\log(\Pr(\text{“obj”} | K, \Theta^*))$$

$$R_p(\text{“bkg”}) = -\log(\Pr(\text{“bkg”} | K, \Theta^*))$$

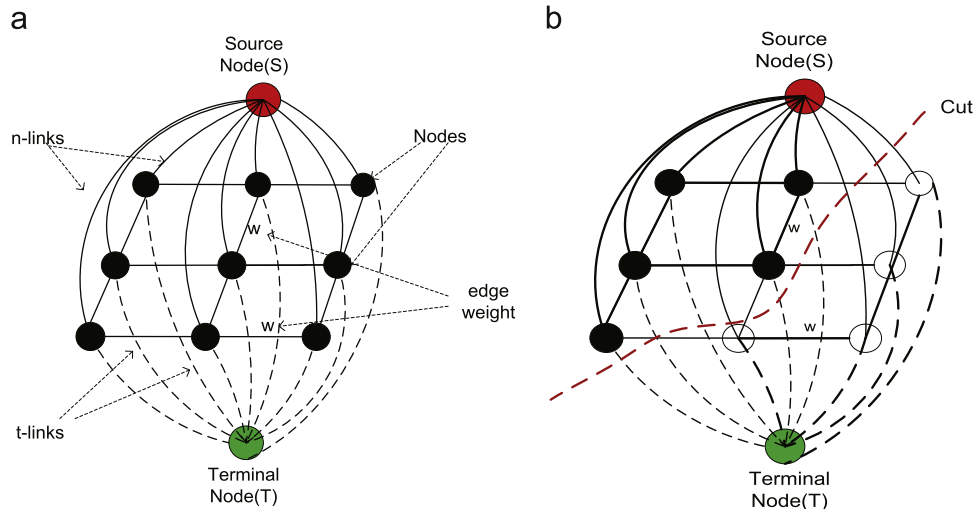


Fig. 2. (a) Corresponding graph of the CT image and (b) resulting cut via minimum cut theory.

Furthermore, the boundary penalty  $B_{\{p,q\}}$  in formula (4) uses an ad hoc function as follows:

$$B_{\{p,q\}} \propto \exp\left(-\frac{(x_p - x_q)^2}{2\sigma^2}\right) \cdot \frac{1}{\text{dist}(p, q)} \quad (8)$$

The energy function of (2) can then be rewritten as follows:

$$E(A, K, \Theta^*) = \lambda \cdot \left\{ -\sum \log(\text{Pr}(A_p | K, \Theta^*)) \right\} + \sum B_{\{p,q\}} \cdot \delta(A_p, A_q) \quad (9)$$

With the region penalty and boundary penalty values, we can create the graph for the CT image (as shown in Fig. 2) and segment using the minimum cut algorithm (1).

### 3. Results and discussion

The data sets of chest CT images used to evaluate the performance of the proposed algorithm were provided by the General Hospital of Ningxia Medical University. The format of the data set is DICOM, and it contains  $512 * 512 * 368 * 16$ -bit images for which the pixel pitch is  $0.74 * 0.74 * 1.0$  mm of each data sets. We implemented our algorithm in C++ programming language based on the max-flow/min-cut code provided by Vladimir Kolmogorov [17] (<http://vision.csd.uwo.ca/code/>). In the experiments, we will investigate the effect of performance on the following aspects: (1) the effect of  $\lambda$  in energy function, (2) the effect of the number  $K$  of GMMs, (3) the comparison of our method with the conventional methods, and (4) the quantitative evaluations.

#### 3.1. The effect of $\lambda$ in energy function

More values in the range  $[0,1]$  for  $\lambda$  were tested in our experiment, and we found out that the changing of  $\lambda$  produces no significant difference in the final segmentation except  $\lambda = 0$ . When  $\lambda = 0$ , there is only the boundary properties in the energy function. With that energy function, our method will be failed to segment the lung parenchyma. And our method will be failed with

the energy function which only has the regional properties part as well. Tested in a relatively large value range of  $\lambda$ , the segmentation accuracy is almost the same. Therefore, we choose  $\lambda = 1$  in our following testing.

#### 3.2. The effect of number $K$ of GMMs

Chen [26] proposed the GrabCut algorithm using the GMM optimization for color image segmentation, and proved the segmentation to be accurate for Gaussian mixture number  $K \geq 5$  and optimal for  $K=7$ . For our lung segmentation task, after tests on some data, we determined that the time consumed for segmentation is higher if  $K$  is higher, refer to Fig. 3. In Fig. 3, the  $K$  is the number of GMMs and  $t$  is the average time consumed for every slice segmentation. Therefore, considering the tradeoff between segmentation accuracy and time cost, we chose  $K=3$  in our experiment. With that value, the boundary of the segmented lung is clear and the segmentation accuracy meets the requirements. Also Fig. 4 presents the results of our proposed method. Here, we show three typical lung CT images, Case 1, Case 2, and Case 3 which are, respectively, the front-end, intermediate, and rear-end layers of lung CT images.

#### 3.3. Compare to the conventional method

In this section, we will give the segmented results of our proposed method compared to the conventional methods. Fig. 5 compares the segmented lung results of the region growing method and the method proposed in this paper. The center images are the segmented results of the region growing method, and the right images are the segmented results of our method. From this figure, we can see that the region growing method always over-segments the lungs, as indicated by the arrows pointing to the main bronchus. With our method, the main bronchus is not segmented out, we do not need the post-processing to remove the bronchus. And Fig. 6 shows the segmented results of lung with juxtapleural lesion via our method compared to the thresholding

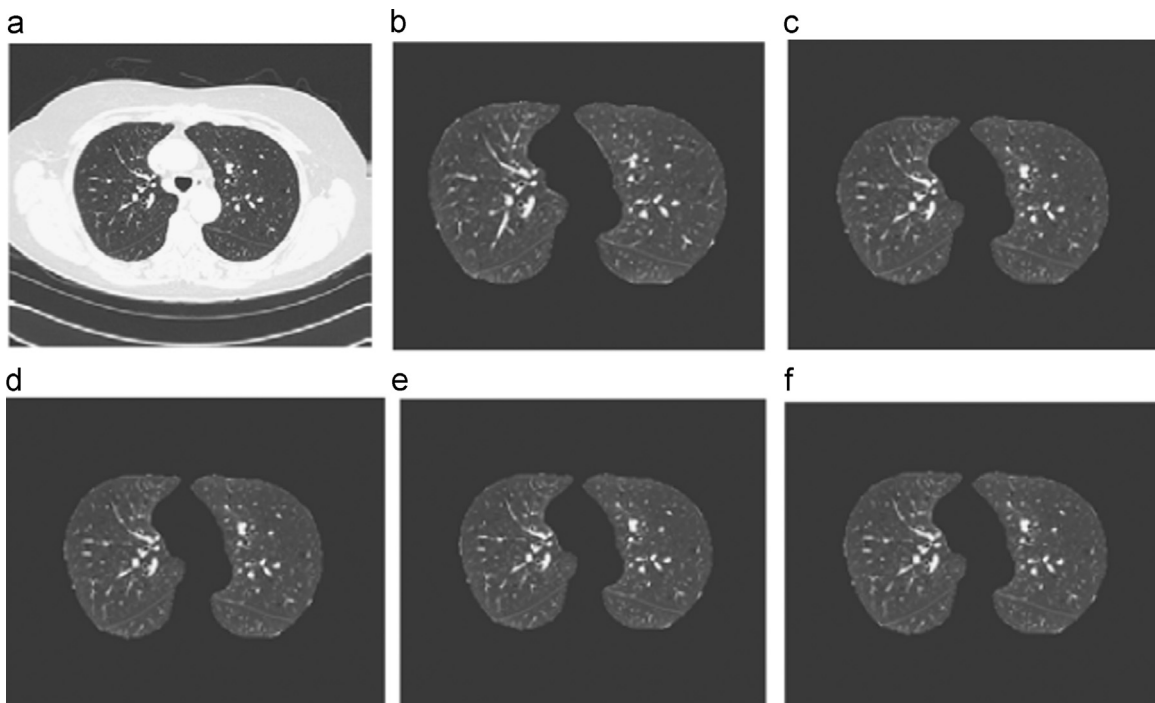
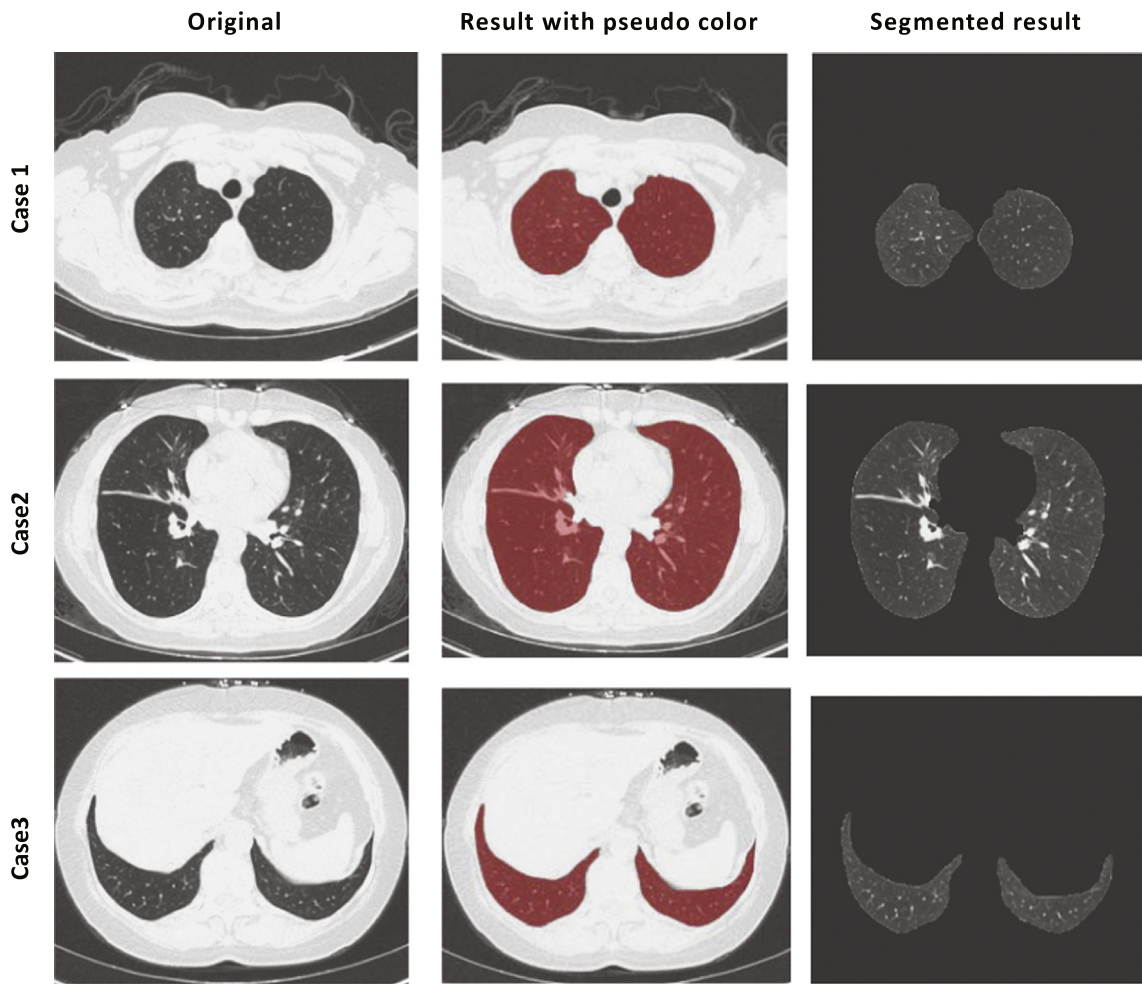
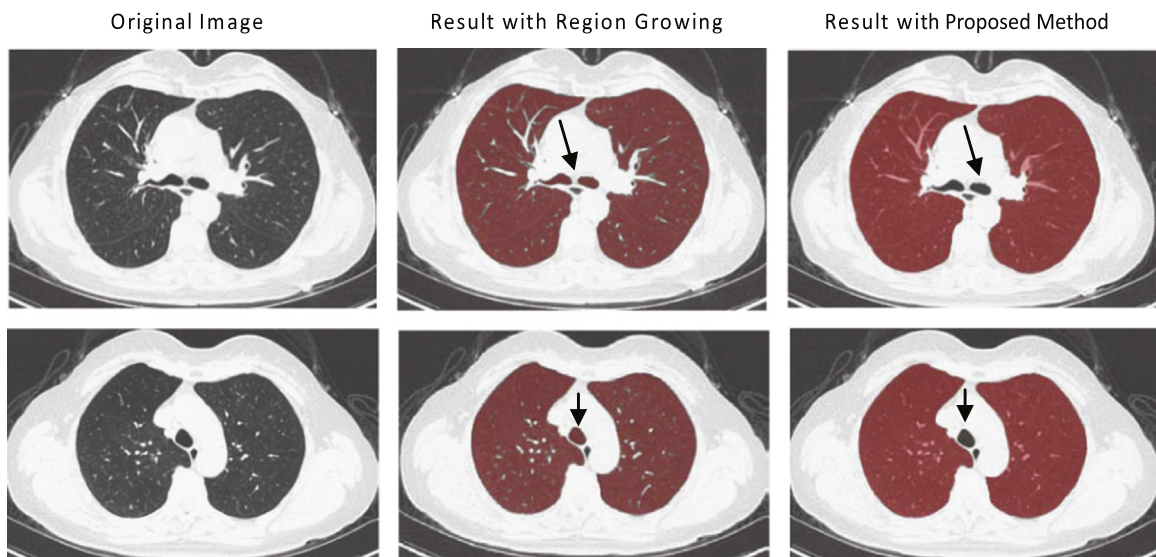


Fig. 3. Segmented lung results using our algorithm. (a) is the original image, and (b)–(f) are the segmented results with a different number  $K$  of GMMs.





**Fig. 4.** Segmented lung results using our algorithm. The left, center, and right columns are the original CT images, segmented results with pseudo-color, and segmented results, respectively.



**Fig. 5.** Comparison of segmentation methods. Original images (left), region growing results (center), and proposed method (right).

method. In Fig. 6, (a) is the original lung CT image, and (b) is the binary image result with the threshold method, (c) is the segmented result with the thresholding method after removing the main bronchus, and (e) and (d) are the results of our method, (e) is

the result with pseudo-color and (d) is the final result. From this figure, we can see that even with the post-processing of removing the main bronchi, the result got from thresholding method has a big hole which is needed to be handled again. However, with our

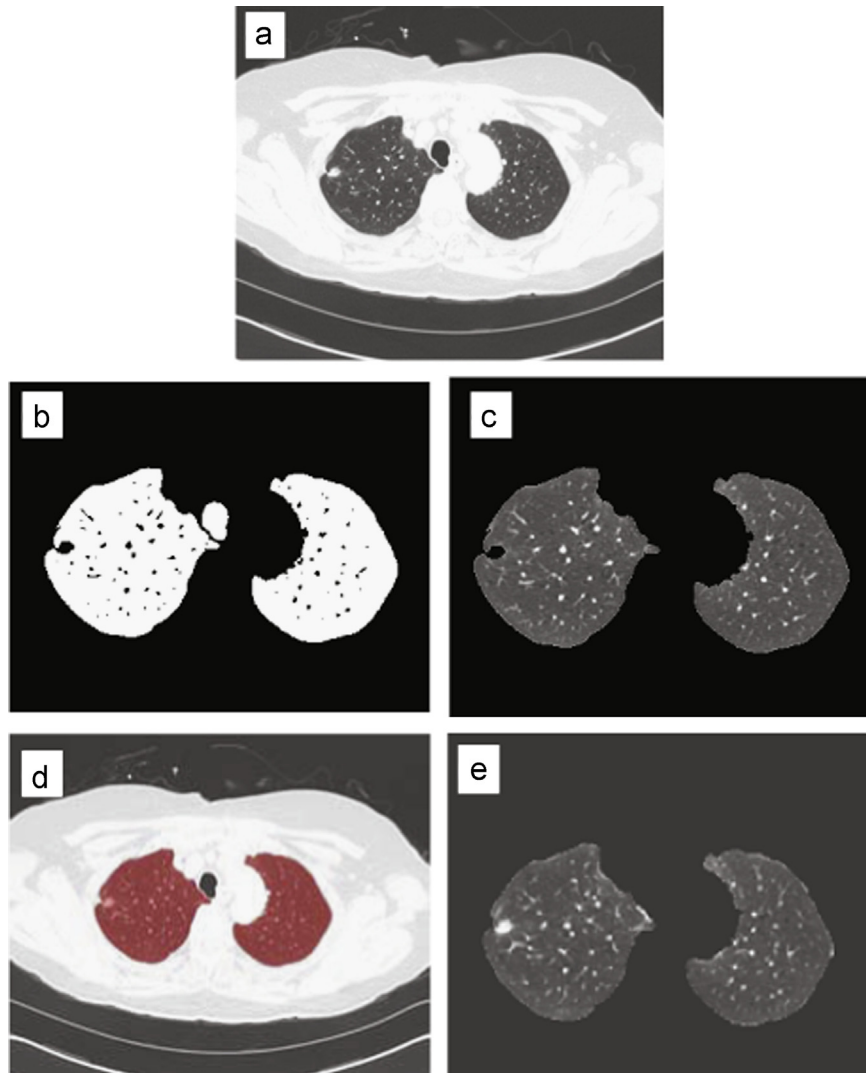


Fig. 6. Compare our proposed method with the thresholding method.

method, the lung regions can be segmented immediately without any post-processing. Though the experimental results show that our proposed method directly provides explicit lung segmentation without any post-processing such as morphological operation, the time consumption is a little higher than both of the thresholding and region growing methods without considering the post-processing operations. As shown in Fig. 3, the average time is about 3 s for one slice segmentation with  $K=3$ , which is an insufficient point in our method.

For some complex scenarios, the left and right lung will be connected to each other after segmented with the conventional algorithms. Then the separation of left and right lung will be needed as a post-processing. But with our method, the left and right lung can be segmented because of the adoption of Gaussian mixture models, as shown in Fig. 7. That is different from the previous methods, and can save the time needed for users to manually separate the two parts of the lung.

### 3.4. Quantitative evaluation

To evaluate the performance of our segmentation approach, we use the Dice similarity coefficient index to quantify the consistency between the segmented results and the gold standard provided by

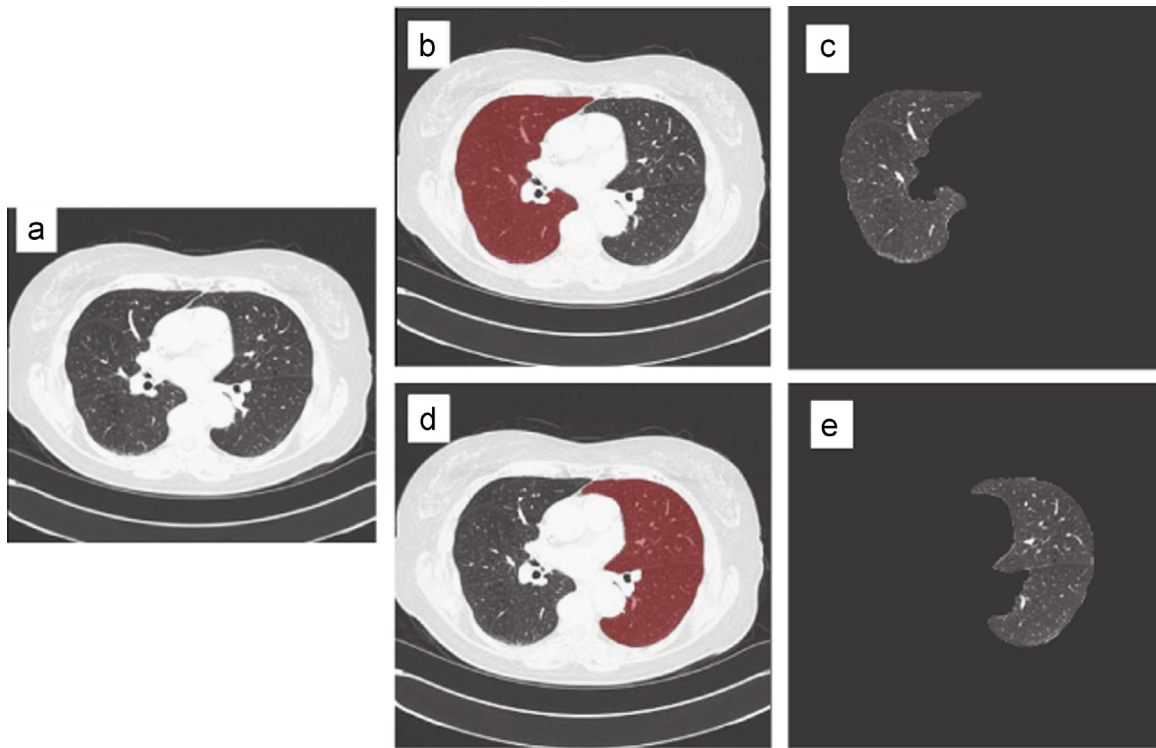
radiologists manually. The Dice coefficient is given by

$$d = 2 * \frac{|R_{seg} \cap R_{gold}|}{|R_{seg}| + |R_{gold}|} \quad (10)$$

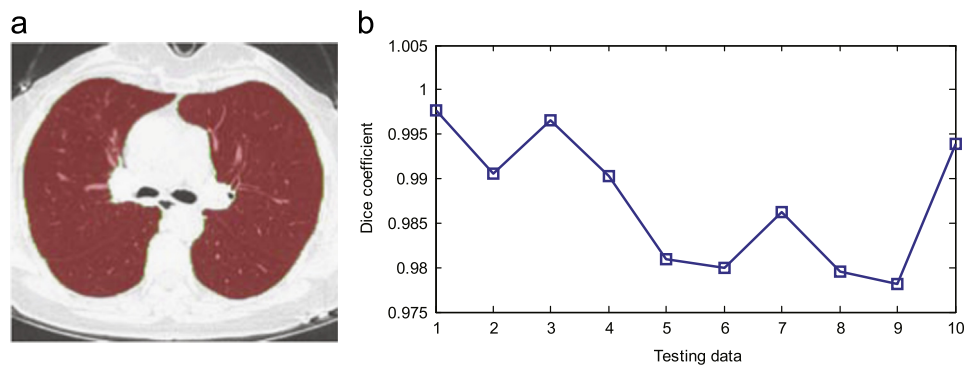
where  $R_{seg}$  is the segmented result of our method, and  $R_{gold}$  is the result segmented by radiologists manually.

Fig. 8(a) shows the result of our proposed method (red pseudo-color) and the manual contours (green lines) delineated by the radiologist on one slice, (b) shows the Dice coefficient index on different CT images. The mean Dice similarity coefficient index for the CT images is approximately 0.9874 with a standard deviation of 0.0070.

Table 1 and Fig. 9 give the comparison between our method and the state of the art works from the quantitative point of view. From Fig. 9, we can see that the Dice similarity coefficient index of our method is higher than that of the method proposed in [18] and a little lower than that of the method proposed in [22], but the running time of our method is longer than that of [18] and much better than that of [22]. Considering the compromise between the accuracy of the segmented results and the computing time of the whole method, we can say that our proposed method is effective and efficient.



**Fig. 7.** (a) Original CT image, (b) segmented right lung with pseudo-color, (c) segmented right lung, (d) segmented left lung with pseudo-color, and (e) segmented left lung.



**Fig. 8.** (a) Automatically segmented results (red pseudo-color) and manual contours (green lines), (b) the Dice coefficients of lungs with our proposed method. (For interpretation of the references to color in this figure caption, the reader is referred to the web version of this paper.)

**Table 1**  
Compared with other methods.

Method	Dice coefficient	Running times (min)
Ref. [18]	0.974	4.5
Ref. [22]	0.9883	15–30
Ours	0.9874	10–15

#### 4. Conclusion

Because of the importance of lung segmentation in lung CT image processing and the clinical analysis of lung disease, research on lung segmentation has received much attention in the past and many segmentation algorithms have been proposed. To facilitate the computer-aided lung lesion treatment planning and quantitative

assessment of lung cancer treatment response, robust lung segmentation method is also needed. The graph cuts algorithm has achieved spectacular progress in computer vision and image processing field, which inspires us to investigate its power in lung segmentation of CT images. In this paper, we present a new method based on graph cuts algorithm improved with GMMs. The experimental results show that our proposed method can directly provide explicit lung segmentation without any post-processing such as morphological operation. And the mean Dice similarity coefficient index for the CT images is approximately 0.9874, the segmentation accuracy and efficiency is significantly improved. However, the time consumption is a little higher, it is about 10–15 min for a whole data set segmentation. All the cost mainly focus on GMMs training process, the construction of corresponding graph and solving of the minimum cut algorithm. So the further optimization on these components will be our future work.



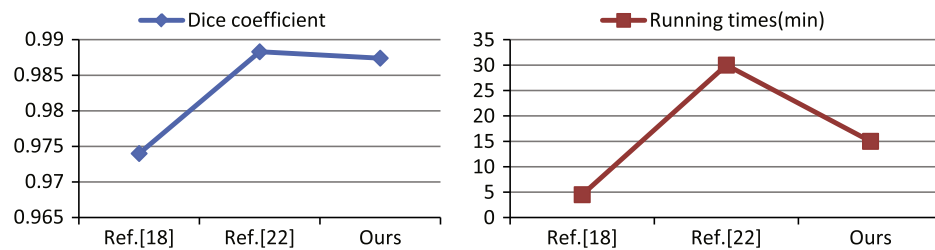


Fig. 9. Compared with other methods.

## Acknowledgments

Thanks to the NSFC (Grant nos. 61271435, U1301251), and Beijing National Science Foundation (No. 4141003) and National Program on Key Basic Research Project (973 Programs) (No. 2011CB706901-4) agency for funding.

## References

- [1] L. Tseng, L. Huang, An adaptive thresholding method for automatic lung segmentation in CT images, in: IEEE AFRICON, 2009, pp. 1–5.
- [2] A. Karthikeyan, M. Vallianmmmai, Lungs segmentation using multi-level thresholding in CT images, *Int. J. Electron. Comput. Sci. Eng.* 1 (3) (2012) 1509–1513.
- [3] H. Gao, L. Dou, The applications of image segmentation techniques in medical CT images, in: Proceedings of the 30th Chinese Control Conference, 2011, pp. 3296–3299.
- [4] Y. Zhang, X. Cheng, Medical image segmentation based on watershed and graph theory, in: 2010 Third International Congress on Image and Signal Processing, 2010, pp. 1419–1422.
- [5] R. Shojaii, J. Alirezaie, P. Babyn, Automatic lung segmentation in CT images using watershed transform, in: IEEE International Conference on Image Processing, vol. 2, 2005, pp. 1266–1270.
- [6] A. Farag, H. Munim, J. Graham, A novel approach for lung nodules segmentation in chest CT using level sets, *IEEE Trans. Image Process.* 22 (12) (2013) 5202–5213.
- [7] J. Lai, M. Ye, Active contour based lung field segmentation, in: International Conference on Intelligent Human–Machine Systems and Cybernetics, 2009, pp. 288–291.
- [8] M. Than, J. Chia, N.M. Noor, Lung segmentation for HRCT thorax images using radon transform and accumulating pixel width, in: 2014 IEEE Region 10 Symposium, 2014, pp. 157–161.
- [9] A. Mansoor, U. Bagci, A generic approach to pathological lung segmentation, *IEEE Trans. Med. Imaging* 33 (12) (2014) 2293–2310.
- [10] L. Meng, H. Zhao, Interactive lung segmentation algorithm for CT chest images based on live-wire model and snake model, in: 2009 International Conference on Electronic Computer Technology, vol. 26, 2009, pp. 461–467.
- [11] J. Pu, J. Roos, C. Yi, Adaptive border marching algorithm: automatic lung segmentation on chest CT images, *Comput. Med. Imaging Graph.* 32 (2008) 452–462.
- [12] S. Sun, C. Bauer, R. Beichel, Automated 3-D segmentation of lungs with lung cancer in CT data using a novel robust active shape model approach, *IEEE Trans. Med. Imaging* 31 (2) (2012) 449–460.
- [13] Y. Boykov, M. Jolly, Interactive graph cuts for optimal boundary and region segmentation of objects in N-D images, in: IEEE International Conference on Computer Vision, vol. 1, 2001, pp. 105–112.
- [14] N. Xu, N. Ahuja, R. Bansa, Object segmentation using graph cuts based active contours, *Comput. Vis. Image Underst.* (2007) 210–224.
- [15] Y. Yang, Q. Liu, H. Liu, L. Yu, F. Wang, Dense depth image synthesis via energy minimization for three-dimensional video, *Signal Process.* 112 (2015) 199–208.
- [16] Y. Yang, X. Wang, Q. Liu, et al. A bundled-optimization model of multiview dense depth map synthesis for dynamic scene reconstruction. *Inf. Sci.*, 2014. <http://dx.doi.org/10.1016/j.ins.2014.11.014>.
- [17] V. Kolmogorov, Y. Boykov, An experimental comparison of min-cut/max-flow algorithms for energy minimization in vision, *IEEE Trans. Pattern Anal. Mach. Intell.* 26 (9) (2004) 1124–1137.
- [18] S. Sun, M. Sonka, R. Beichel, Graph-based 4D lung segmentation in CT images with expert-guided computer-aided refinement, in: IEEE 10th International Symposium on Biomedical Imaging, 2013, pp. 1312–1315.
- [19] B. Price, B. Morse, S. Cohen, Geodesic graph cut for interactive image segmentation, in: IEEE conference on Computer Vision and Pattern Recognition, 2010, pp. 3161–3168.
- [20] C. Ballangan, X.Y. Wang, M. Fulham, S. Eberl, D.D. Feng, Lung tumor segmentation in PET images using graph cuts, *Comput. Methods Prog. Biomed.* 109 (3) (2013) 260–268.
- [21] A.M. Ali, A.S. El-Baz, A.A. Farag, A novel framework for accurate lung segmentation using graph cuts, in: The Fourth IEEE International Symposium on Biomedical Imaging: From Nano to Macro, 2007, pp. 908–911.

- [22] K. Nakagomi, A. Shimizu, H. Kobatake, M. Yakami, K. Fujimoto, K. Togashi, Multi-shape graph cuts with neighbor prior constraints and its application to lung segmentation from a chest CT volume, *Med. Image Anal.* 17 (1) (2013) 62–77.
- [23] J. Liu, H. Zhang, Image segmentation using a local GMM in a variational framework, *J. Math. Imaging Vis.* 46 (2) (2013) 161–176.
- [24] R. Farnoosh, B. Zarpak, Image segmentation using Gaussian mixture model, *IJST Int. J. Eng. Sci.* 19 (1) (2008) 29–32.
- [25] Y.M. Qin, G.R. Weng, Lung nodule segmentation using EM algorithm, in: The Sixth International Conference on Intelligent Human–Machine Systems and Cybernetics, 2014, pp. 20–23.
- [26] D. Chen, B. Chen, Improved grabcut segmentation via GMM optimisation, in: IEEE Digital Image Computing: Techniques and Applications (DICTA), 2008, pp. 39–45.



**Shuangfeng Dai** received the B.S. degree in Automatic, in 2003, and the M.S. degree in Control Theory and Control Engineer, in 2006, both from the Yanshan University in Qinhangdao, China. Currently, she is working towards the Ph.D. degree in University of Chinese Academy of Sciences. Her research interests include medical image segmentation and 3D–4D image visualization.



**Ke Lu** was born in Guyuan Ningxia on March, 1971. He graduated from Department of Mathematics at Ningxia University, in July 1993. He received Master degree and Ph.D. degree from Department of Mathematics and Department of computer science at Northwest University, in July 1998 and July 2003, respectively. He is a Postdoctoral Fellow in Institute of Automation Chinese Academy of Sciences from July 2003 to April 2005. Currently he is a Professor of University of the Chinese Academy of Sciences. His research focuses on curve matching, 3D image reconstruction and computer graphics.



**Jiyang Dong** was born in 1990. He received the B.S. degree in electronics engineering from Tsinghua University, Beijing, China, in 2008. He is currently pursuing the Ph.D. degree in digital image processing with the University of Chinese Academy of Science, Beijing. His current research interests include medical image segmentation and image registration.



**Yifei Zhang** was born in 1990. He received the B.S. degree in electronics engineering from Tsinghua University, Beijing, China, in 2008. He is currently pursuing the M.S. degree in digital image processing with the University of Chinese Academy of Science, Beijing. His current research interests include remote image processing and computer vision.





**Yong Chen** was born in Shandong Province in 1969. He graduated at Ningxia Medical University, in July 1993. He received master degree at Ningxia University, in June 2008. Currently he is a Professor of Graduate University of the Ningxia Medical University. His research focuses on functional image in CT and MRI.